Bioorganic & Medicinal Chemistry Letters 26 (2016) 328–333

Contents lists available at ScienceDirect

Bioorganic & Medicinal Chemistry Letters

journal homepage: www.elsevier.com/locate/bmcl

Development and structural analysis of adenosine site binding tankyrase inhibitors

Teemu Haikarainen [a,†], Jo Waaler [b,†], Alexander Ignatev [a], Yves Nkizinkiko [a], Harikanth Venkannagari [a], Ezeogo Obaji [a], Stefan Krauss [b,*], Lari Lehtiö [a,*]

[a] Faculty of Biochemistry and Molecular Medicine and Biocenter Oulu, University of Oulu, Oulu, Finland
[b] Unit for Cell Signaling, Institute of Medical Microbiology, Oslo University Hospital, Gaustadalleen 34, 0372 Oslo, Norway

ARTICLE INFO

Article history:
Received 9 November 2015
Revised 1 December 2015
Accepted 7 December 2015
Available online 8 December 2015

Keywords:
ARTD
PARP
Tankyrase
Tankyrase inhibitor
WNT signaling
WNT inhibitor
Small-molecule

ABSTRACT

Tankyrases 1 and 2, the specialized members of the ARTD protein family, are druggable biotargets whose inhibition may have therapeutic potential against cancer, metabolic disease, fibrotic disease, fibrotic wound healing and HSV viral infections. We have previously identified a novel tankyrase inhibitor scaffold, JW55, and showed that it reduces mouse colon adenoma formation in vivo. Here we expanded the scaffold and profiled the selectivity of the compounds against a panel of human ARTDs. The scaffold also enables a fine modulation of selectivity towards either tankyrase 1 or tankyrase 2. In order to get insight about the binding mode of the inhibitors, we solved crystal structures of the compounds in complex with tankyrase 2. The compounds bind to the adenosine pocket of the catalytic domain and cause changes in the protein structure that are modulated by the chemical modifications of the compounds. The structural analysis allows further rational development of this compound class as a potent and selective tankyrase inhibitor.

Tankyrase 1 (TNKS1/PARP-5a/ARTD5) and tankyrase 2 (TNKS2/PARP-5b/ARTD6) are protein modifying enzymes, which have recently been in the focus of intense search for specific inhibitors. Tankyrases are composed of multiple protein domains and share a catalytic ARTD domain responsible for poly(ADP-ribosyl)ation of target proteins, a SAM domain involved in tankyrase oligomerization, and ankyrin repeats which mediate interactions with other proteins. Tankyrases regulate the stability of target proteins by binding to a specific motif and attaching poly(ADP-ribose) chains to the target protein. The poly(ADP-ribose) chain serves as a recognition site for the E3 ubiquitin ligase RNF146 that induces ubiquitination leading to proteasomal degradation.[1,2]

The most extensively studied pathways in which tankyrases have been shown to elicit a regulatory function are centriole elongation and mitotic spindle formation, telomere cohesion, exocytosis of IRAP and GLUT4 containing trans-Golgi vesicles and the WNT/β-catenin signaling pathway.[3–16]

Here we studied a recently identified tankyrase inhibitor JW55 (**1**)[15] and its analogs. We used a cell-based SuperTOP-Luciferase/Renilla (ST-Luc/Ren) reporter assay to screen compounds for their inhibition of canonical WNT/β-catenin signaling. With a biochemical assay we confirmed that the analogs specifically inhibit tankyrases and profiled the selectivity of the compounds against eight other human ARTDs. To provide structural insights on their inhibitory mechanism, we determined crystal structures of the most potent analogs and the parent compound **1** in complex with TNKS2 and show that the inhibitors anchor to the adenosine subsite of the donor NAD^+ binding groove. The structures explain the high selectivity of the scaffold and provide further routes for enhancing compound potency.

The primary hit **1** moderately inhibited tankyrases and WNT/β-catenin signaling.[15] A selection of JW55 (**1**) analogs (Table 1) were tested for their ability to inhibit β-catenin-mediated canonical WNT signaling at various compound concentrations. This ST-Luc/Ren assay was performed using a WNT3a-induced and stably transfected HEK293 cell line (ST-Luc/Ren HEK293), as reported earlier.[14,17] In vitro inhibition, as measured by biochemical assay complemented the ST-Luc/Ren assay, showed moderate potency of **1** towards tankyrases (TNKS1 IC_{50} 1.80 μM, TNKS2 IC_{50} 2.01 μM, ST-Luc/Ren IC_{50} 1.23 μM), which is in agreement with a previously measured value by an independent biochemical activity assay.[15]

Compounds based on the core structure **1** with substitutions at the furan ring exhibited modest improvements on inhibiting canonical WNT/β-catenin signaling as compared to **1** (Table 1).

* Corresponding authors.
E-mail addresses: stefan.krauss@rr-research.no (S. Krauss), lari.lehtio@oulu.fi (L. Lehtiö).
† These authors contributed equally.

http://dx.doi.org/10.1016/j.bmcl.2015.12.018
0960-894X/

Substituting the furan group with a 4-methoxyphenyl group led to **2** and improved the cellular IC_{50} to 0.79 μM. Interestingly, **2** is a selective inhibitor of TNKS2 with IC_{50} 0.26 μM but has poor potency towards TNKS1 (IC_{50} 11 μM). Despite this isoform selectivity **2** stabilized AXIN1 and destabilized non-phoshorylated β-catenin moderately better than **1** in both HEK293 cells and SW480 cells (Fig. 1). Substituting the furan group with 2-methylfuran led to **3** and gave an improved cellular IC_{50} of 0.38 μM (TNKS1 IC_{50} 0.69 μM; TNKS2 IC_{50} 2.30 μM). Altering the central *p*-phenylene ring of **1** to a 2-chloro-*p*-phenylene led to **4** and showed a cellular IC_{50} of 0.38 μM (TNKS1 IC_{50} 0.57 μM; TNKS2 IC_{50} 2.15 μM). Substituting the furan group in **4** with a 2-methyl oxazole gave **5** but did

Table 1
JW55 analogs as tankyrase inhibitors

	Compound	IC_{50} (pIC_{50} ± SEM)		ST-Luc/Ren IC_{50} ± SDM (μM)	PDB code
		TNKS1	TNKS2		
1	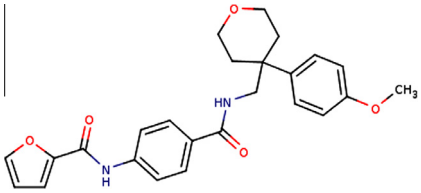	1.80 μM (5.74 ± 0.10)	2.01 μM (5.70 ± 0.12)	1.23 ± 0.60	5ADQ
2	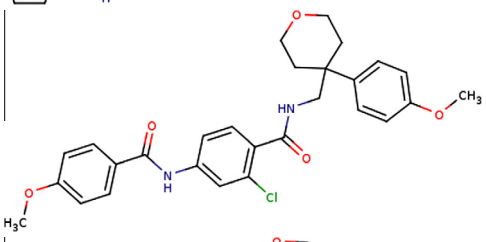	11.08 μM (4.96 ± 0.05)	0.26 μM (6.59 ± 0.19)	0.79 ± 0.05	ND
3	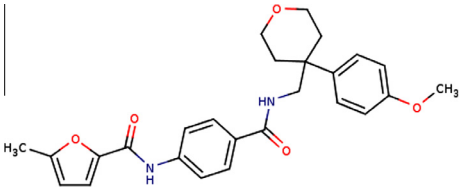	0.69 μM (6.16 ± 0.02)	2.30 μM (5.64 ± 0.21)	0.38 ± 0.20	5ADR
4	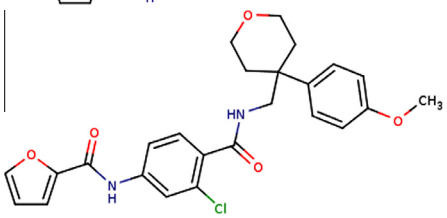	0.57 μM (6.25 ± 0.03)	2.15 μM (5.67 ± 0.07)	0.36 ± 0.10	5ADS
5	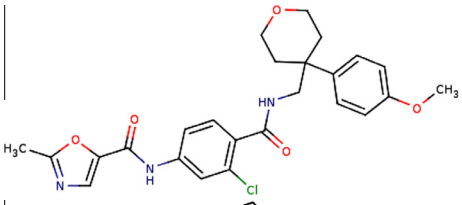	1.13 μM (5.95 ± 0.18)	2.23 μM (5.65 ± 0.09)	0.69 ± 0.04	5ADT
6	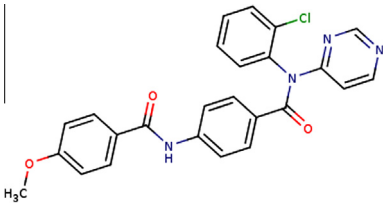	0.55 μM (6.26 ± 0.09)	0.037 μM (7.43 ± 0.08)	1.91 ± 0.10	5AEH
7	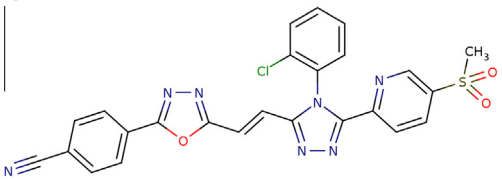	0.046 μM ± 0.001	0.025 μM ± 0.006	0.05 ± 0.02	4HYF

Biochemical IC_{50} and corresponding pIC_{50} ± SEM (n = 3) and ST-Luc/Ren IC_{50} ± SDM are reported. Data for **7** is from Voronkov and co-workers and ± SDM is shown for both biochemical and ST-Luc/Ren data.[17]

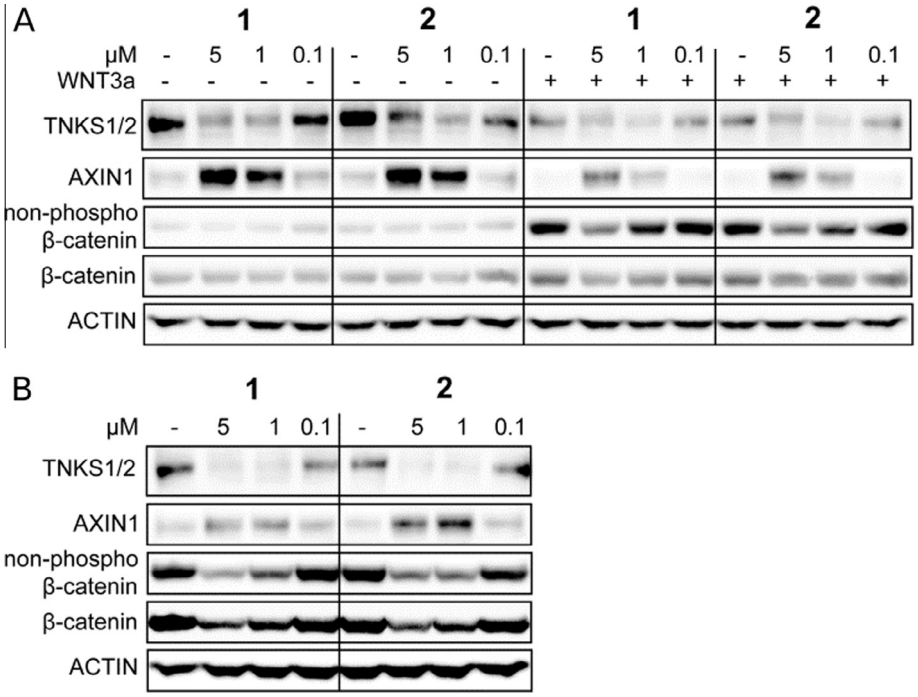

Figure 1. Western blot analysis shows that both **1** and **2** dose-dependently (24 h incubation) mediate decreased TNKS1/2 abundance, increased AXIN1 stability and in addition degradation of active (non-N terminal phosphorylated) and total β-catenin in (A) WNT3a-stimulated (+) HEK293 cells and (B) APC-mutated SW480 CRC cells. Compound treatment concentrations (μM) are indicated while the corresponding controls are in 0.1% DMSO (−). ACTIN antibody documents equal protein loading. The blots show representative data derived from multiple experiments.

Table 2
Profiling **4** and **6** against a panel of human ARTDs

Compound	IC_{50} (μM)							
	ARTD1	ARTD2	ARTD3	ARTD4	ARTD7	ARTD8	ARTD10	ARTD12
4	>100	>100	>100	>100	>10[a]	>10[a]	>10[a]	>10[a]
6	77	>100	>100	>100	>10[a]	>10[a]	>10[a]	>10[a]

[a] Limited by assay DMSO tolerance.

not show improvements and led to a cellular IC_{50} of 0.69 μM (TNKS1 IC_{50} 1.13 μM; TNKS2 IC_{50} 2.23 μM).

The weak biochemical potency of **2** towards TNKS1 prompted us to measure the alterations in the protein amounts of tankyrase, the tankyrase target and structural protein of the β-catenin degradasome AXIN1, along with the mediator of canonical WNT signaling β-catenin using Western blot analysis. Wild type HEK293 cells and SW480 cells were incubated with **1** and **2** at various concentrations for 24 h. The analysis confirmed that the observed ST-Luc/Ren inhibition in HEK293 cells can be rationalized by tankyrase inhibition also with **2** as it results in (i) altered levels of TNKS1/2, (ii) increased AXIN1 abundance and (iii) decreased quantities of non-phosphorylated and transcriptional active β-catenin (Fig. 1). Interestingly, treatment with **1** and **2** decreased protein levels of both TNKS1 and TNKS2 upon treatment in the two cell lines. This observation is opposite to the observed stabilization of these two proteins after treatment with the tankyrase inhibitor XAV939.[4]

A more radical change of the structure of the molecule, retaining the core structure from **2**, which showed the highest selectivity to TNKS2 in an enzymatic assay and combining N-(2-chlorophenyl) and pyrimidine groups based on SAR studies of **7** (G007-LK)[17,18] yielded the most potent compound (TNKS1 IC_{50} 0.55 μM; TNKS2 IC_{50} 0.037 μM) that still retained a moderate preference to inhibiting TNKS2. However, the cellular IC_{50} (1.91 μM) was reduced when compared with the control compound **7** (Table 1).

The selectivity of **4** and **6** were tested with eight other ARTDs, namely ARTD1, 2, 3, 4, 7, 8, 10, and 12 (Table 2). The compounds displayed high selectivity for tankyrases and had negligible inhibition over the other ARTD enzymes tested.

The binding modes of **1** and analogs **3**, **4**, **5**, and **6** were analyzed by soaking them to crystals of the TNKS2 ARTD domain. The catalytic domains of TNKS1 and 2 have 94% sequence identity with all the residues conserved in the donor NAD^+ binding site.[19] Despite multiple attempts, we were unable to soak **2** to crystals. The compounds bind to the adenosine subsite of the donor NAD^+ binding groove and induce an opening of the D-loop lining the site (Fig. 2).

Binding of the compounds **1**, **3**, **4**, and **5** is largely mediated by hydrophobic interactions. The tetrahydropyran rings of the compounds extend towards the nicotinamide site and are lined by hydrophobic Ile1051, Gly1053, Tyr1060, Tyr1071, and Ile1075 (Fig. 2a–d). The 4-methoxyphenyl moiety of the compounds is situated in a hydrophobic pocket between F- and G-loops lined by Ser1033, Pro1034, Phe1035, Ile1051, and Ile1075. The aromatic furan ring is bound between an α-helix containing hydrophobic Ala1038 and Ile1039 and to His1048 from the D-loop. The compounds are almost parallel with His1048 forming a stacking interaction with it.

1, **3**, **4**, and **5** form two hydrogen bonds to the main chain amides of Tyr1060 and Asp1045 via their carbonyl oxygens. Similar

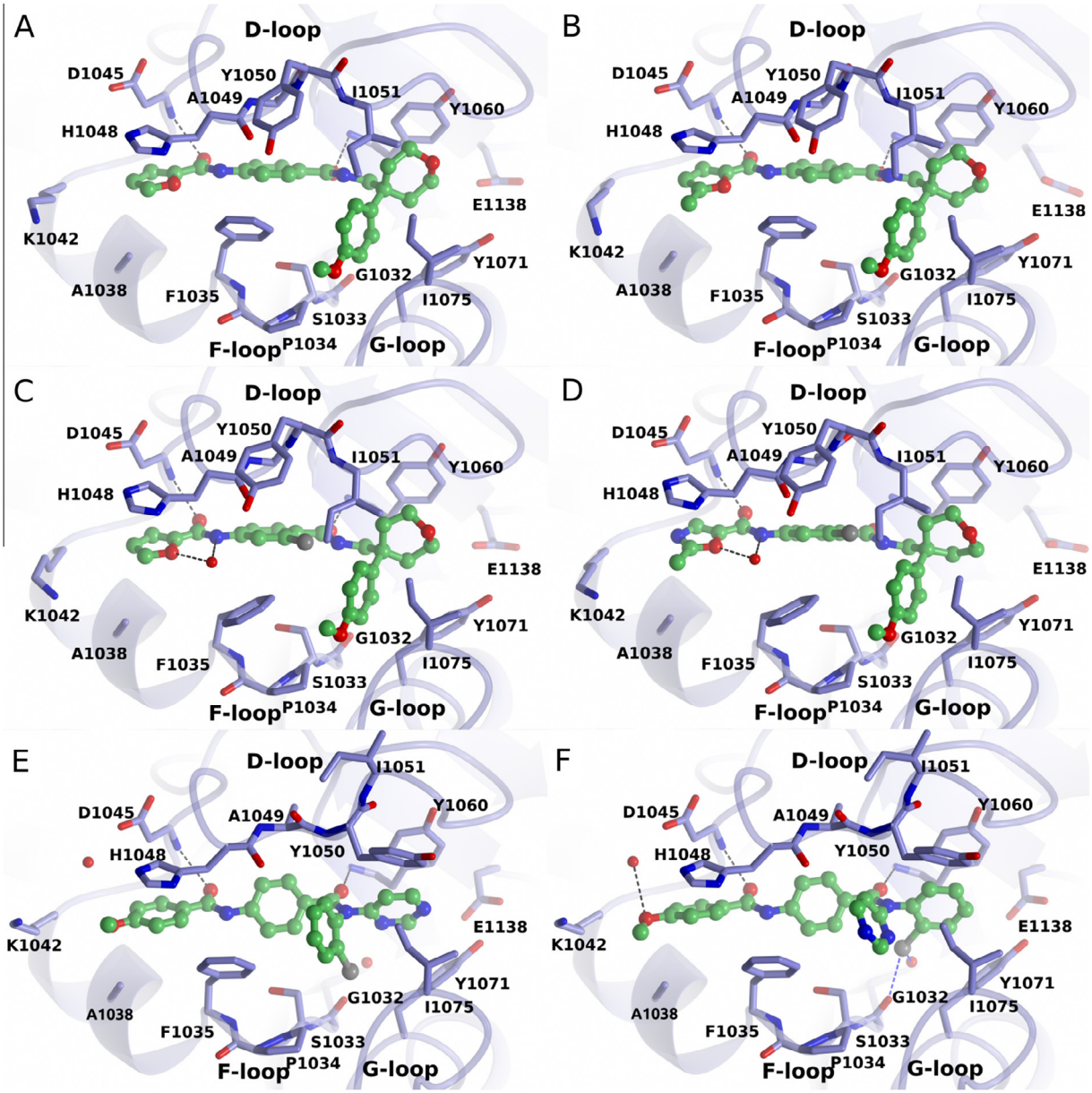

Figure 2. Co-crystal structures of the inhibitors with the catalytic domain of TNKS2: (A) **1**, (B) **3**, (C) **4**, (D) **5**, (E) **6** conformation 1, and (F) **6** conformation 2. Hydrogen bonds are displayed as black dotted lines. Halogen bonds in (F) are depicted as blue dotted lines.

interactions are also present in the other inhibitors binding to this site, namely WIKI4, IWR-1, and G007-LK.[17,20,21]

Despite similar structures there are some differences in the binding modes of **3**, **4**, and **5** when compared to **1**. The methyl substitution in the furan ring of **3** does not induce large changes in the binding mode when compared to **1** (Fig. 2a and b). However, it allows for more efficient hydrophobic interactions with the binding site namely with Phe1035, Ala1038 and Lys1042. In **4**, the substitution of the chlorine in the central phenyl group causes a shift in the position of the D-loop in (Fig. 2c). Ile1051 moves 1.1 Å closer to the compound, and Tyr1050 is pushed 0.9 Å away from the binding site. Interestingly, **4** induces a 75° turn of Phe1035 at the opposing F-loop allowing a water molecule to bind between the inhibitor and the residue. Compound **5** shares the methyl and chlorine substitutions of **3** and **4**, respectively. However, it has lowered potency compared to the two compounds, most likely due to the amide substitution in the furan ring, which disturbs the hydrophobic interactions made by the ring with Lys1042 (Fig. 2d).

Compound **6** binds to the same pocket in the TNKS2 catalytic domain (Fig. 2e and f). Similarly to the JW55 analogs the compound forms mainly hydrophobic interactions with the protein, but also the two hydrogen bonds to Asp1045 and Tyr1060 are present. Notably, the **6** is bound in two conformations in the crystal structure with equal occupancy. The difference between two conformers is a rotation of pyrimidinyl and chlorophenyl groups around the amide bond in a way that the aromatic rings switch places in the binding pocket. In the first conformation (Fig. 2e) chlorophenyl adopts a similar conformation as seen previously for **7** (Supplementary Fig. 1).[17] In the second conformation (Fig. 2f), the compound forms a halogen bond with Gly1032 and a water molecule located near the nicotinamide binding site, and an additional hydrogen bond is formed between the oxygen of methoxyphenyl group and a water molecule. Additional substitutions in

these aromatic rings could stabilize one of the conformations. Pyrimidinyl (conformation 1) and chlorophenyl (conformation 2) groups are π-stacking against Tyr1060. In contrast to other compounds the shorter linker between pyrimidinyl/chlorophenyl and central benzene ring causes an almost 90° rotation of latter due to steric clashes. Binding of **6** causes changes in the D-loop. Ile1051 is moved out from the binding site and is not involved in interactions. Tyr1050 instead, moves towards the compound forming additional hydrophobic interactions. Interestingly, the larger methoxyphenyl substitution does not induce major changes compared to the furan and oxazole analogs. Only Lys1042 is moved away from the compound although this residue is not well ordered in the crystal structure.

Compounds based on the JW55 scaffold share similar interactions as other recently published inhibitors binding to the adenosine subsite of tankyrases.[17,21] Inhibitors are selective towards tankyrases over eight other ARTD isoenzymes tested and thus the scaffold adds further chemical space to develop specific tankyrase inhibitors. Structural studies of the JW55 scaffold implicated several possible routes to further improve the potency of these inhibitors. Other inhibitors binding to this site contain bigger substitution in the place of the furan ring which forms parallel stacking interaction with His1048. The substitution of the small aromatic furan with larger ring systems would be a logical starting point to further improve compound potency. JW55 and WIKI4 both contain a methoxyphenyl moiety extending towards the G-loop. However, because of slightly different orientation of the group, the oxygen of the methoxy group can interact with the backbone amide of Ile1075 in case of WIKI4.[21] Other hydrophilic substitutions at the place of the methoxy group could be tested in order to form an interaction with Ile1075. The tetrahydropyran ring extending towards the nicotinamide binding site is close to several potential hydrogen bond donors and acceptors that may be addressed. These include the carbonyl oxygen of Ile1051 and amides of Met1054 and Gly1053 as well as hydroxyl of Tyr1071.

The compounds generally had similar potencies towards both tankyrase isoforms. However, **2** displayed a ≈40-fold selectivity towards TNKS2 in the enzymatic activity assay. Although we were not able to get a crystal structure of the TNKS2-**2** complex, there are no structural differences between TNKS1 and 2, which could explain the TNKS2 selectivity of the compound. Also **6** displayed ≈15-fold selectivity towards TNKS2. Both compounds **2** and **6** share an *m*-methoxyphenyl group. Isoform selectivity at this range has been previously observed for tankyrase inhibitors, although a comprehensive rationale for tankyrase isoform selectivity is currently lacking.[22–26] Most likely differences in the dynamics of the donor NAD^+ binding sites between the isoforms lead to the observed differences in the potencies. However, despite the differential biochemical selectivity of **2** to TNKS2, the effect of **2** on protein stability was similar in the cellular assay and in the same dose range as the effect of compound **1** (**1** showed no significant selectivity to either tankyrases). These data indicate functional redundancy of both tankyrase in the context of AXIN stabilization and β-catenin turnover.

Despite the moderate potency of the chemotype, its high target selectivity along with promising in vitro as well as in vivo tumor inhibition data[15] demonstrates that the compound scaffold has potential to be developed further towards a functional tankyrase and WNT inhibitor for research and clinical purposes. We have studied the detailed binding modes of the inhibitor series using protein crystallography and could therefore provide initial structure activity relationship for structure-based design. Inhibitors binding to the adenosine subsite display a high selectivity towards tankyrases making this class of inhibitors attractive to further development. Merging of the features from **1** and **7** was successful and yielded a compound **6** which is a potent and selective tankyrase inhibitor. Structure–activity relationship data of both compounds can now be combined in order to improve the cellular potency of this chimeric scaffold.

Accession codes: Coordinates and structure factors have been deposited to the protein data bank with codes 5ADQ, 5ADR, 5ADS, 5ADT, and 5AEH for TNKS2-**1**, TNKS2-**3**, TNKS2-**4**, TNKS2-**5**, and TNKS2-**6**, respectively.

Acknowledgments

This work was carried out with the support of the Diamond Light Source (Didcot, UK) and the European Synchrotron Radiation Facility (ESRF, Grenoble, France). We are grateful to Local Contacts at ESRF and at Diamond for providing assistance in using beamlines ID14-1 and I04-1. The use of the facilities and expertise of the Biocenter Oulu core facility, a member of Biocenter Finland and Instruct-FI, is gratefully acknowledged.

The work was funded by Biocenter Oulu, Sigrid Jusélius Foundation and Jane and Aatos Erkko Foundation. T.H. is supported by the Academy of Finland (grant no. 266922). J.W is supported by the Research Council of Norway and the Norwegian Cancer Society grant N° 5803958-2014. The research leading to these results has received funding from the European Community's Seventh Framework Program (FP7/2007-2013) under BioStruct-X (grant agreement N° 283570).

Supplementary data

Supplementary data (contains experimental procedures, as well as crystallographic data collection, processing, and refinement statistics) associated with this article can be found, in the online version, at http://dx.doi.org/10.1016/j.bmcl.2015.12.018.

References and notes

1. Callow, M. G.; Tran, H.; Phu, L.; Lau, T.; Lee, J.; Sandoval, W. N.; Liu, P. S.; Bheddah, S.; Tao, J.; Lill, J. R.; Hongo, J.-A.; Davis, D.; Kirkpatrick, D. S.; Polakis, P.; Costa, M. *PloS One* **2011**, *6*, e22595.
2. Zhang, Y.; Liu, S.; Mickanin, C.; Feng, Y.; Charlat, O.; Michaud, G. A.; Schirle, M.; Shi, X.; Hild, M.; Bauer, A.; Myer, V. E.; Finan, P. M.; Porter, J. A.; Huang, S.-M. A.; Cong, F. *Nat. Cell Biol.* **2011**, *13*, 623.
3. Kim, M. K.; Smith, S. *Mol. Biol. Cell* **2014**, *25*, 30.
4. Huang, S.-M. A.; Mishina, Y. M.; Liu, S.; Cheung, A.; Stegmeier, F.; Michaud, G. A.; Charlat, O.; Wiellette, E.; Zhang, Y.; Wiessner, S.; Hild, M.; Shi, X.; Wilson, C. J.; Mickanin, C.; Myer, V.; Fazal, A.; Tomlinson, R.; Serluca, F.; Shao, W.; Cheng, H.; Shultz, M.; Rau, C.; Schirle, M.; Schlegl, J.; Ghidelli, S.; Fawell, S.; Lu, C.; Curtis, D.; Kirschner, M. W.; Lengauer, C.; Finan, P. M.; Tallarico, J. A.; Bouwmeester, T.; Porter, J. A.; Bauer, A.; Cong, F. *Nature* **2009**, *461*, 614.
5. Haikarainen, T.; Krauss, S.; Lehtio, L. *Curr. Pharm. Des.* **2014**, *20*, 6472.
6. Yeh, T.-Y. J.; Beiswenger, K. K.; Li, P.; Bolin, K. E.; Lee, R. M.; Tsao, T.-S.; Murphy, A. N.; Hevener, A. L.; Chi, N.-W. *Diabetes* **2009**, *58*, 2476.
7. Chi, N. W.; Lodish, H. F. *J. Biol. Chem.* **2000**, *275*, 38437.
8. Guo, H.-L.; Zhang, C.; Liu, Q.; Li, Q.; Lian, G.; Wu, D.; Li, X.; Zhang, W.; Shen, Y.; Ye, Z.; Lin, S.-Y.; Lin, S.-C. *Cell Res.* **2012**, *22*, 1246.
9. Kim, M. K.; Dudognon, C.; Smith, S. *EMBO Rep.* **2012**, *13*, 724.
10. Dynek, J. N.; Smith, S. *Science* **2004**, *304*, 97.
11. Ozaki, Y.; Matsui, H.; Asou, H.; Nagamachi, A.; Aki, D.; Honda, H.; Yasunaga, S. 'ichiro; Takihara, Y.; Yamamoto, T.; Izumi, S.; Ohsugi, M.; Inaba, T. *Mol. Cell* **2012**, *47*, 694.
12. Hsiao, S. J.; Smith, S. *Biochimie* **2008**, *90*, 83.
13. Chang, P.; Coughlin, M.; Mitchison, T. J. *Mol. Biol. Cell* **2009**, *20*, 4575.
14. Waaler, J.; Machon, O.; von Kries, J. P.; Wilson, S. R.; Lundenes, E.; Wedlich, D.; Gradl, D.; Paulsen, J. E.; Machonova, O.; Dembinski, J. L.; Dinh, H.; Krauss, S. *Cancer Res.* **2011**, *71*, 197.
15. Waaler, J.; Machon, O.; Tumova, L.; Dinh, H.; Korinek, V.; Wilson, S. R.; Paulsen, J. E.; Pedersen, N. M.; Eide, T. J.; Machonova, O.; Gradl, D.; Voronkov, A.; von Kries, J. P.; Krauss, S. *Cancer Res.* **2012**, *72*, 2822.
16. Zhong, L.; Yeh, T.-Y. J.; Hao, J.; Pourtabatabaei, N.; Mahata, S. K.; Shao, J.; Chessler, S. D.; Chi, N.-W. *PloS One* **2015**, *10*, e0122948.
17. Voronkov, A.; Holsworth, D. D.; Waaler, J.; Wilson, S. R.; Ekblad, B.; Perdreau-Dahl, H.; Dinh, H.; Drewes, G.; Hopf, C.; Morth, J. P.; Krauss, S. *J. Med. Chem.* **2013**, *56*, 3012.
18. Lau, T.; Chan, E.; Callow, M.; Waaler, J.; Boggs, J.; Blake, R. A.; Magnuson, S.; Sambrone, A.; Schutten, M.; Firestein, R.; Machon, O.; Korinek, V.; Choo, E.; Diaz, D.; Merchant, M.; Polakis, P.; Holsworth, D. D.; Krauss, S.; Costa, M. *Cancer Res.* **2013**, *73*, 3132.

19. Lehtiö, L.; Collins, R.; van den Berg, S.; Johansson, A.; Dahlgren, L.-G.; Hammarström, M.; Helleday, T.; Holmberg-Schiavone, L.; Karlberg, T.; Weigelt, J. *J. Mol. Biol.* **2008**, *379*, 136.
20. Narwal, M.; Venkannagari, H.; Lehtiö, L. *J. Med. Chem.* **2012**, *55*, 1360.
21. Haikarainen, T.; Venkannagari, H.; Narwal, M.; Obaji, E.; Lee, H.-W.; Nkizinkiko, Y.; Lehtiö, L. *PLoS One* **2013**, *8*, e65404.
22. Larsson, E. A.; Jansson, A.; Ng, F. M.; Then, S. W.; Panicker, R.; Liu, B.; Sangthongpitag, K.; Pendharkar, V.; Tai, S. J.; Hill, J.; Dan, C.; Ho, S. Y.; Cheong, W. W.; Poulsen, A.; Blanchard, S.; Lin, G. R.; Alam, J.; Keller, T. H.; Nordlund, P. *J. Med. Chem.* **2013**, *56*, 4497.
23. Haikarainen, T.; Narwal, M.; Joensuu, P.; Lehtiö, L. *ACS Med. Chem. Lett.* **2014**, *5*, 18.
24. Shultz, M. D.; Cheung, A. K.; Kirby, C. A.; Firestone, B.; Fan, J.; Chen, C. H.-T.; Chen, Z.; Chin, D. N.; Dipietro, L.; Fazal, A.; Feng, Y.; Fortin, P. D.; Gould, T.; Lagu, B.; Lei, H.; Lenoir, F.; Majumdar, D.; Ochala, E.; Palermo, M. G.; Pham, L.; Pu, M.; Smith, T.; Stams, T.; Tomlinson, R. C.; Touré, B. B.; Visser, M.; Wang, R. M.; Waters, N. J.; Shao, W. *J. Med. Chem.* **2013**, *56*, 6495.
25. Paine, H. A.; Nathubhai, A.; Woon, E. C. Y.; Sunderland, P. T.; Wood, P. J.; Mahon, M. F.; Lloyd, M. D.; Thompson, A. S.; Haikarainen, T.; Narwal, M.; Lehtiö, L.; Threadgill, M. D. *Bioorg. Med. Chem.* **2015**, *23*, 5891.
26. Kumpan, K.; Nathubhai, A.; Zhang, C.; Wood, P. J.; Lloyd, M. D.; Thompson, A. S.; Haikarainen, T.; Lehtiö, L.; Threadgill, M. D. *Bioorg. Med. Chem.* **2015**, *23*, 3013.